

## **General Disclaimer**

### **One or more of the Following Statements may affect this Document**

- This document has been reproduced from the best copy furnished by the organizational source. It is being released in the interest of making available as much information as possible.
- This document may contain data, which exceeds the sheet parameters. It was furnished in this condition by the organizational source and is the best copy available.
- This document may contain tone-on-tone or color graphs, charts and/or pictures, which have been reproduced in black and white.
- This document is paginated as submitted by the original source.
- Portions of this document are not fully legible due to the historical nature of some of the material. However, it is the best reproduction available from the original submission.

NASA CR-145087

ACOUSTICAL EVALUATION OF THE NASA  
LANGLEY V/STOL WIND TUNNEL

By

István L. Vér

(NASA-CR-145087) ACOUSTICAL EVALUATION OF  
THE NASA LANGLEY V/STOL WIND TUNNEL (Bolt,  
Beranek, and Newman, Inc.) 45 p  
HC A05/MF A01

N77-11068

CSCI 20A

Unclas  
54533

G3/09



Prepared under Contract No. NAS1-9559  
Task Order No. 13

By

BOLT BERANEK AND NEWMAN INC.  
50 Moulton Street  
Cambridge, Massachusetts 02138



National Aeronautics and  
Space Administration

Langley Research Center  
Hampton, Virginia 23665  
AG 24 827-3906

**Page intentionally left blank**

## TABLE OF CONTENTS

	<u>page</u>
LIST OF FIGURES .....	iv
SECTION I. SUMMARY .....	1
SECTION II. DESCRIPTION OF THE TUNNEL .....	4
SECTION III. ACOUSTICAL ENVIRONMENT .....	5
SECTION IV. SELF NOISE IN THE OPEN TEST SECTION .....	7
A. Ambient Noise in the Open Test Section ..	7
B. Self-Noise with the Ground Belt <sup>®</sup> Operational .....	8
C. Self-Noise with the Boundary Layer Suction Fan Operational .....	8
D. Self-Noise with the Tunnel Fan Operational .....	9
SECTION V. SPATIAL DISTRIBUTION OF THE SOUND FIELD IN THE OPEN TEST SECTION .....	12
SECTION VI. IMPULSE RESPONSE MEASUREMENTS .....	16
SECTION VII. PREREQUISITES FOR PERFORMING VALID ACOUSTICAL MEASUREMENTS IN THE OPEN TUNNEL TEST SECTION.	20
SECTION VIII. OBSERVATIONS MADE WITH THE CLOSED TEST SEC- TION CONFIGURATION .....	23
SECTION IX. RECOMMENDATIONS .....	25
REFERENCES .....	26

## LIST OF FIGURES

	<u>page</u>
Figure 1. Plan view of the V/STOL Wind Tunnel .....	27
2. Octave band spectrum of the ambient noise in the open test section with tunnel fan stationary ...	28
3. Octave band spectrum of the ground belt system measured at 3 ft from the downstream end of the belt .....	29
4. Octave band spectrum of the boundary layer suction fan noise in the open test section with the tunnel fan stationary .....	30
5. Comparison of the fan noise levels in the test section measured in and out of the stream .....	31
6. Comparison of the fan noise levels measured in the stream by two different microphones .....	32
7. Octave band spectrum of the driving fan noise in the tunnel test section measured with the porous pipe microphone with air speed as parameter .....	33
8. Normalized octave band sound pressure level of the V/STOL and full-scale wind tunnels due to the operation of driving fans .....	34
9. Example for the evaluation of the hall radius from measured SPL vs distance curves by the best-fit method .....	35
10. Hall radius of the open test section for the various directions .....	36
11. Distribution of the normalized sound pressure level vs distance data in the open tunnel test section for all frequencies and all directions .	37
12. Impulse response of the open tunnel test section measured in the 63-Hz center frequency octave band .....	38

LIST OF FIGURES (*Continued*)

	<u>page</u>
Figure 13. Impulse response of the open tunnel test section recorded in the 500-Hz and 4000-Hz center frequency octave bands .....	39
14. Initial reverberation times measured with various source and receiver locations .....	40
15. SPL vs distance measured in the downstream direction in the closed V/STOL Tunnel .....	41
16. SPL vs distance measured in the upstream direction in the closed V/STOL Tunnel .....	42

## I. SUMMARY

This report presents the results of the acoustical measurements made by BBN under Task Order No. 13 of the Master Agreement NAS1-9559 at the NASA Langley Research Center's V/STOL Wind Tunnel. The purpose of these measurements was to supply NASA Langley operating personnel with the acoustical characteristics of the tunnel test section needed for the planning of acoustical measurements and to identify the major noise sources. Although the contract called for only the acoustical evaluation of the open test section configuration, we also performed some preliminary measurements in the closed tunnel configuration. The series of measurements performed included:

1. Evaluation of the octave band ambient noise level in the open test section with the tunnel fan stationary.
2. Evaluation of the octave band noise level in the open test section for various settings of the boundary layer suction fan with the tunnel fan stationary.
3. Evaluation of the octave band noise level of the boundary layer belt for various belt speeds with the tunnel fan stationary.
4. Evaluation of the octave band noise level of the driving fan in the open tunnel test section as a function of the air speed.
5. Mapping of the sound field of an omnidirectional sound source of known acoustical power output in the open tunnel test section with tunnel fan stationary.
6. Measurement of the impulse response in the open test section and in certain other locations in the tunnel with no airflow.
7. Preliminary measurements of the spatial distribution of sound in the closed tunnel with no airflow.

Analysis of the measured data indicates that the open test section of the V/STOL Wind Tunnel has potential as an environment for performing certain types of acoustical measurements. However, the validity of the test results will depend upon the acoustical power output, the radiation pattern, the frequency spectrum and the dimensions of the sound source investigated, the distance between source and microphone, and the directivity and air flow noise rejection capability of the microphone used. Accordingly, there are practical limitations in the acoustical testing which can be performed. The data presented in this report provide the information necessary for planning such testing so that the results will be valid.

Since the boundaries of the open tunnel test section have widely differing acoustical characteristics, its room acoustic is very complex, as is clearly indicated by both the impulse response and spatial distribution of the sound field. The reverberant sound field in the open test section is far from being diffuse. This nondiffuse nature of the reverberant sound field does not permit the usual determination of the sound power output of an unknown source from the space-averaged sound pressure measured in the reverberant field.

The sound power output and directivity pattern of noise sources located in the open tunnel test section can be determined only by measuring the intensity of the direct sound. In order that the microphone measure the true pressure of the direct sound, the sound pressure of the reverberant field, the pressure fluctuations generated by the airflow, and the sound pressure due to the operation of the various equipment (such as driving fan, boundary layer suction fan, ground belt, etc.), must be small compared with the sound pressure of the direct sound at all microphone locations.



Increasing the efficiency of the already present sound absorbing treatment on the interior wall surfaces by removing the impervious surface layer, reducing the noise output of the boundary layer suction fan, and using special directive microphones with an ability to cancel the effect of flow noise are the measures to be taken to increase the radius within which meaningful acoustical measurements can be performed.

The results of our preliminary measurements of the spatial distribution of the sound field in the closed tunnel configuration indicate that the total sound power output of an unknown sound source placed in the test section could most probably be evaluated by measuring the sound pressure in two properly chosen locations in the duct - one upstream and one downstream of the test section. However, we recommend that the practicability of this method of sound power output measurements be further investigated, preferably in a small scale model of the V/STOL Tunnel. The results of such a model study would be generally applicable to all closed circuit wind tunnels.

## II. DESCRIPTION OF THE TUNNEL

A plan view of the NASA Langley Research Center's V/STOL Wind Tunnel is shown in Fig. 1. The closed circuit tunnel is driven by a nine-blade propeller of 40-ft diameter powered by an 8000 hp AC motor capable of providing an air speed of 250 mph in the test section at 275 rpm. The length of the closed loop is 770 ft.

To simulate takeoff and landing conditions, the test section is equipped with a boundary layer suction fan and a ground belt. The boundary layer suction fan removes the turbulent boundary layer built up on the tunnel floor before it enters the test section. Because the ground belt runs at the same speed as the air, a new build-up of the turbulent boundary layer is prevented. The boundary layer suction is used up to 89 mph air speed ( $Q=20 \text{ lb/ft}^2$ ), while the maximum speed of the ground belt is only 34 mph. So that the airflow in the test section is homogeneous and low in turbulence, the tunnel cross section at the upstream turning vane is large compared with the cross section of the test section. In addition, a diffusing screen is placed between the upstream turning vane and the test section to break up any remaining turbulence. The tunnel test section can be used either in closed or in open configuration. The closed test section is 14.5 ft wide, 21.75 ft high, and approximately 70 ft long. The open test section configuration is achieved by lifting the walls and ceiling of the test section enclosure up above the air stream. In this case, the air stream is surrounded by the stationary air in the large room enclosing the test section.

### III. ACOUSTICAL ENVIRONMENT

Sound generation by aerodynamic processes, such as vortex shedding of propellers, is an area where experimental research is needed. For such aerodynamic processes, the presence of the DC airflow simulating the forward speed of the aircraft may considerably influence the sound power output of the source.

Since one can simulate real-life conditions much better in the test section of V/STOL Tunnel, where the DC flow can be conveniently provided, than in stationary whirl towers, the acoustical environment of the test section is of particular interest to NASA personnel who plan to carry out such experimental research.

Unfortunately, the V/STOL Tunnel was not designed to be used for acoustical measurements. The auxiliary equipment is noisy, and there is no silencer or sound absorbing treatment in the path of air circulation which would attenuate fan noise before it could enter the test section. Although the interior wall surfaces of the test section enclosure are lined with a 2 in. thick glass fiber blanket, an impervious layer of plastic, which serves to protect it, renders it acoustically ineffective, especially at high frequencies.

The acoustically advantageous features of the tunnel are the low tip speed of the driving fan (tip Mach number 0.5 at maximum rpm) and the beneficial location of the fan relative to the test section (i.e., they are separated by two 90° bends). Due to these acoustically advantageous features, the noise level of the driving fan measured in the open test section of the V/STOL Tunnel for a given air speed is still considerably lower than in the test section of the full-scale tunnel, where there is line-of-sight between the driving fan and test platform [1].

Because of the widely differing sound absorption characteristics of the room boundaries, the sound field in the open test section is very complex. Sound waves radiated in the upstream and downstream direction enter the ducts and build up a reverberant field there which, in turn, feeds sound energy back into the test section. Sound waves radiated toward the walls of the test section enclosure are partly absorbed and partly reflected by the wall, while those radiated in the vertical direction practically become trapped between the floor and the raised ceiling of the test section. The presence of these two hard parallel surfaces favors the buildup of standing waves and explains why the hall radius measured in the vertical direction is substantially smaller than that measured in other directions. Because of these nonisotropic acoustical properties of the test section, there is no simple way to relate the space-averaged sound pressure level measured in the reverberant field of the open test section to the sound power output of the radiating sound source. Accordingly, the sound power output of the source must be determined by measuring the direct sound. The presence of the reverberant sound field, the self-noise of the tunnel, and the flow-induced pressure fluctuations, which interfere with the proper measurement of the direct sound, set the lower limit of the sound power output of a source which can be evaluated in the test section of the V/STOL Tunnel.

The next section deals with that equipment which contributes to the self-noise of the V/STOL Tunnel.

#### IV. SELF NOISE IN THE OPEN TEST SECTION

The self noise of the V/STOL tunnel is the sum of the ambient noise determined by intruding construction noise, aircraft noise, and the noise of such auxiliary equipment as the boundary layer suction fan, ground belt drive, driving fans of the tunnel, air conditioning, leaky valves, etc.

##### A. Ambient Noise in the Open Test Section

Figure 2 shows the octave band spectrum of the ambient noise measured in the open test section with the tunnel fan, the boundary layer suction fan and the ground belt stationary.

The upper curve corresponds to the normal condition when the chiller, the oil circulating pump, and the air conditioning system are operational. The middle curve was obtained when the chiller and air conditioning system were shut off but the pump was still operational. The lowest noise levels represented by the lower curve in Fig. 2 were obtained when the chiller, air conditioning and pump were shut off. Except in the 4000-Hz and 8000-Hz center frequency octave bands where the ambient noise is controlled by leaky valves and gaskets, this curve represents the lowest noise level which can be achieved in the open test section without airflow. With proper noise control of the pump, the chiller, and the air conditioning system, the noise level in the open test section could be lowered by approximately 10 dB. Since the self-noise of the operational tunnel, even at low airspeeds, is expected to be above the normal ambient noise, such noise control measures will be required only if the open test section of tunnel is planned to be used for acoustical measurements without airflow.

## B. Self-Noise with the Ground Belt Operational

The test section of the V/STOL Tunnel is equipped with a ground belt which runs at the same velocity as the air stream to simulate actual landing and takeoff conditions. Figure 3 shows the octave band spectrum of the noise level measured at 3 ft from the downstream edge of the ground belt as a function of the belt speed with the tunnel fan stationary. Due to the smooth running of the belt, the noise level is only slightly higher than the noise level of the cooling fan.

Because the noise of the driving fans at the same air speed always exceeds the noise of the ground belt system, it is not necessary to reduce the belt noise.

## C. Self-Noise with the Boundary Layer Suction Fan Operational

To remove the turbulent boundary layer which builds up on the tunnel floor upstream of the test section, the V/STOL Tunnel is equipped with a powerful suction fan taking in air through a slot running across the test section just upstream of the ground belt. The air intake duct does not have any acoustical treatment so that the fan noise enters the test section without attenuation. Figure 4 shows the octave band spectrum of the space-averaged sound pressure level in the test section for various typical operating conditions (i.e., dial settings 9.4, 7.3, 6.4 and 4 and the corresponding pressure readings of 41.5, 41.5, 37.5 and 33.5 in. H<sub>2</sub>O) of the boundary layer suction fan. The noise levels are excessively high, even exceeding the level of the driving fan noise. At a boundary layer gauge setting of

6.4 and pressure gauge reading of 37.5 in.  $H_2O$ , we observed very disturbing resonance effects manifesting themselves in very high sound pressure levels in the 31.5 Hz and 63 Hz center frequency octave bands (see Fig. 4). Though our instruments did not have the capability of measuring much below 20 Hz, our observations indicate that there is a considerable amount of energy in pulsations at frequencies even lower than 20 Hz.

Since this high intensity noise of the boundary layer suction fan not only will interfere with planned acoustical measurements in the tunnel test section, but also will interfere seriously with the activities of the operating personnel in the control room, *the noise control of the boundary layer suction fan should have the highest priority.*

#### D. Self-Noise with the Tunnel Fan Operational

Except in the case when the boundary layer suction fan is used, the noise level in the open test section of the operational tunnel is controlled by the driving fan and the noise created by the interaction of the flow with solid boundaries. Our observations in this tunnel and in other wind tunnels [1] indicate that propeller noise dominates the noise created by the flow passing the turning vanes. The octave band spectrum of the fan noise in the test section was measured simultaneously by three microphones as a function of the air speed. A Bruel & Kjaer 1-in. microphone with nose cone [2] and a specially developed porous-pipe microphone [3] were placed in the center of the air stream. Figure 5 shows the levels measured by these two microphones after applying the proper corrections for frequency response and directivity. At low frequencies, up to 125 Hz, both microphones in the stream

measure the same noise level. Above 125 Hz, the Bruel & Kjaer microphone with nose cone measures levels which are as much as 10 dB higher than that measured by the porous-pipe microphone. The higher levels measured by the nose cone type microphone are due to the sensitivity of this microphone to flow-induced noise. This conclusion can be proven indirectly by comparing the noise levels measured by the porous pipe microphone in the stream with that measured by a random incidence microphone outside of the stream as shown in Fig. 6. Except at the high frequency end of the spectrum, where the microphone outside of the stream did not have line-of-sight\* to the upstream nozzle, there is good agreement between the two sets of data. This agreement proves that the porous-pipe, due to its ability to reject aerodynamically induced noise, was measuring the true sound pressure in the stream and that the microphone with nose cone was limited by flow noise. Accordingly, the noise levels measured by the porous-pipe microphone have been used to evaluate the flow speed dependence of the driving fan noise in the open test section. Figure 7 shows the octave band spectrum of the driving fan noise measured in the middle of the stream for various air speeds. Analyzing the measured data in Fig. 7, we found that, as in the case of the full-scale tunnel [1], the octave band spectrum of the driving fan noise scales with the sixth power of the air speed. The data points tend to collapse if normalized as

$$SPL_N (\text{OCT}) = SPL (\text{OCT}, U_{\text{mph}}) - 60 \log_{10} (U_{\text{mph}}) \quad (1)$$

where  $SPL_N (\text{OCT})$  is the normalized octave band sound pressure

---

\*At low tunnel speeds, where it was possible to place the microphone in a position just out of the stream with line-of-sight to the nozzle, good agreement was also found at high frequencies.



level given in Eq. 1,  $SPL(OCT, U_{mph})$  is the octave band sound pressure level measured in the open test section at an air speed of  $U_{mph}$ , and  $U_{mph}$  is the tunnel speed normalized to 1 mph.

Figure 8 shows the range and average value of the normalized octave band sound pressure level of the V/STOL Tunnel's open test section. Because the octave band sound pressure level in the test section, if normalized according to Eq. 1, seems to be an appropriate measure to characterize the self-noise for any wind tunnel, Fig. 8 also shows the respective normalized octave band spectrum of the Full-Scale Wind Tunnel for comparison. As expected, the V/STOL Tunnel, where the driving fan does not have direct line-of-sight to the test section, has a lower normalized sound pressure level spectrum than does the Full-Scale Tunnel where the driving fan is located directly downstream of the tunnel test section and has direct line-of-sight to the test platform.

Considering the excellent correlation of the driving fan noise with the sixth power of the air speed, it is proposed that the normalized sound pressure level, as defined in Eq. 1, should be evaluated for various subsonic wind tunnels to rank order them with respect to self-noise.

## V. SPATIAL DISTRIBUTION OF THE SOUND FIELD IN THE OPEN TEST SECTION

In a well-behaved room where the sound absorbing element is evenly distributed on the various wall surfaces, the sound pressure in the reverberant field  $p_{rev}$  and the sound power output of the source  $W_0$  are related by Eq. 2.

$$\overline{p_{rev}^2} = \frac{4\rho_0 c_0}{S\bar{\alpha} + 4mV} W_0, \quad (2)$$

where  $\rho_0 c_0$  is the characteristic impedance of the air;  $S$  is the total interior surface area,  $\bar{\alpha}$  is the average energy absorption coefficient of the wall surfaces,  $m$  is the air absorption coefficient which depends on frequency and relative humidity [4], and  $V$  is the room volume.

In the direct field where the intensity of the direct sound is much larger than that of the reverberant sound, the sound pressure  $p(r)$  as a function of the distance from the acoustical center  $r$  is given by [1]

$$p(r, \phi, \theta) = \left[ \frac{W_0 \rho_0 c_0 e^{-\alpha r} Q(\phi, \theta)}{4\pi r^2} \right]^{\frac{1}{2}}, \quad (3)$$

where  $Q(\phi, \theta)$  is the directivity factor of radiation, defined as the ratio of the sound intensity measured in the direction defined by the polar and elevation angles  $\phi$  and  $\theta$  to the intensity which would be measured at the same distance for an omnidirectional source of the same power output.

The distance where the sound pressure of the direct field equals the sound pressure of the reverberant field, the so-called hall radius  $r_H$ , is obtained by combining Eqs. 2 and 3, yielding

$$r_H = \left[ \frac{Q(\phi, \theta) (S\bar{\alpha} + 4mV) e^{-r_H^m}}{16\pi} \right]^{\frac{1}{2}} \quad (4)$$

Since the sound field in the open test section of the V/STOL Tunnel is far from being diffuse, the hall radius cannot be calculated from Eq. 4, which is valid only for the diffuse case.

To obtain a measure for the extent of the area where the direct field of an omnidirectional source dominates the reverberant field, we measured the sound pressure level vs distance curves of a semi-omnidirectional sound source of known power output. We used a loudspeaker system consisting of a regular twelve-sided polyhedron with an 8-in. diameter Altec 409 B speaker mounted in each face as a semi-omnidirectional source. This loudspeaker system was constructed and calibrated by Mr. Paul T. Soderman of NASA Ames\*. A detailed description of the source and calibration data can be found in Ref. 5. The dodecahedron sound source hung 7 ft and 10 in. above the floor near the center of the test section. The microphone was supported on a tripod 3½ ft above floor level. The sound source was fed by octave bands of white noise. The voltage at the output terminals of the power amplifier was kept 8 V<sub>rms</sub> for each octave band. The sound field in the north, east,

---

\* The author would like to thank Mr. Soderman for making this calibrated sound source available for this program.

south, west, and vertical directions were sampled at different distances. In analyzing the measured results, we first normalized the octave band sound pressure levels to  $10^{-12}$  watt source power according to

$$\text{SPL}_n(r) = \text{SPL}(r) - \text{PWL} \quad , \quad (5)$$

where  $\text{SPL}_n(r)$  is the sound pressure level in dB re 0.0002  $\mu\text{bar}$  measured in distance  $r$ , and PWL is the power level of the source in dB re  $10^{-12}$  watts. These normalized sound pressure levels then were plotted as a function of distance for each octave band for the various directions. As an example, Fig. 9 shows the normalized sound pressure level vs distance curve of the west traverse measured in the 2000-Hz center frequency octave band.

Figure 10 shows the hall radius vs frequency curve obtained from the measured data for the different directions. As expected, the smallest hall radius is obtained from the vertical traverse, because of the presence of the two hard parallel surfaces (i.e., the tunnel floor and the raised ceiling panel), favoring the build up of standing waves between these surfaces. The experimentally evaluated hall radius peaks in the 250-Hz center frequency octave band where the sound absorption of the walls is maximum.

To find an average value for the hall radius and gain some information about the magnitude of scatter, we plotted the data points for all directions and for all frequency bands (see Fig. 11). Considering the interference between the sound waves which reach the microphone by the direct path and those reflected

from the hard floor [4], the scatter is not excessive. In the direct field the data points closely cluster around the theoretical value indicating that our sound source was omnidirectional and properly calibrated. The average value of the hall radius from Fig. 11 is 16 ft, which agrees well with the data presented in Fig. 10.

## VI. IMPULSE RESPONSE MEASUREMENTS

To provide the dynamic range necessary for proper evaluation of the impulse response, we used a small 10 gauge cannon as an impulsive-sound source. The first series of impulse responses were recorded with both the 10 gauge cannon and the microphone located at different points inside of the open tunnel test section. The recorded impulse responses have been analyzed in octave bands. Figure 12 shows a typical impulse response obtained in the 63-Hz center frequency octave band. It shows deterministic fluctuations. The average time interval between the successive peaks of the filtered impulse response closely corresponds to the time required for the sound wave to run once forth and back between the microphone and the raised ceiling panel (i.e.,  $2 \times 21.5$  ft), indicating the existence of a flutter echo between the two hard, flat, parallel surfaces constituted by the floor and the raised ceiling panel. It is reasonable to assume that the small hall radius measured in the vertical direction is due to the presence of this flutter echo. No distinct reflections have been observed from areas of the tunnel outside of the test section.

Starting in the 125-Hz center frequency octave band where the wavelength of the sound becomes small compared with the dimensions of the duct cross section, the impulse response of the open tunnel test section exhibits a pronounced peak which occurs 0.35 seconds after the arrival of the direct sound, indicating that a substantial percentage of the sound energy entering the downstream duct through the shroud is reflected back into the open test section from the flat rigid duct wall at the first elbow. (The 0.35 second transit time closely corresponds to this distance.) The upper graph in Fig. 13 is

representative for the type of decay curves obtained in the frequency range between 125 Hz and 2000 Hz. Before the arrival of the reflected sound from the first downstream turn, the open tunnel test section remains isolated from the rest of the tunnel, and the sound decays at a fast rate which is determined by the sound absorption of the interior wall surfaces and by the power loss through the shroud and nozzle openings.

After the arrival of the first reflected sound wave from the downstream elbow, the duct starts to feed energy back into the open test section. From this time on, the sound pressure in the test section decays at the slower rate characteristic of the lightly damped resonances of the air enclosed in the duct. It should be noted that the amplitude of the reflected wave for certain combinations of microphone and cannon locations in the test section was only 2 to 3 dB lower than the amplitude of the direct sound, especially in the 125-Hz center frequency band where the reflection is most intense. In the 2000-Hz center frequency octave band, the reflection is barely noticeable; in the 4000-Hz center frequency octave, as shown in the lower curve in Fig. 13, one notices only a change in slope, indicating that 0.35 sec. after the arrival of the direct sound the ducts start to feed energy back into the open test section, and the decay rate becomes substantially smaller than during the first 0.35 sec. The transit time of sound through the closed duct loop is 0.63 sec. The recorded impulse response curves did not show at this time interval any obvious peaks which would indicate a strong circulation of sound energy.

The initial reverberation time of the open test section was evaluated from the average slope of the decay curves in the first 0.35 sec for the various octave bands and is plotted

as the lowest curve in Fig. 14. The reverberation time is high at low frequencies, reaches a minimum in the 250-Hz and 500-Hz center frequency bands and increases again with increasing frequency up to 4000 Hz. In the 8000-Hz center frequency band, it decreases slightly due to air absorption.

To study the mechanism of the power transfer between the sound field in the highly reverberant duct spaces and the more sound absorbing open test section, we made a second set of impulse response measurements with the cannon located in the duct near the downstream turning vane (Pos. 2 in Fig. 1) and the microphone in the open test section. The reverberation times of this configuration, evaluated in octave bands, are plotted in Fig. 14. Since in this case all the sound energy supplied to the test section must come from the highly reverberant duct spaces, the microphone in the open test section registered reverberation times as much as an order of magnitude higher than in the case when the cannon have been located in the test section.

For the third set of impulse response measurements, both the cannon and the microphone were located inside of the duct near the first downstream turning vane (i.e., in Pos. 2) to record the impulse response of the reverberant duct space. The reverberation times of the duct space as a function of frequency have been evaluated from the filtered decay rate curves, and are also plotted in Fig. 14. Comparing the two upper curves, one finds that the reverberation times of the open test section are very similar to the reverberation times of the duct spaces, if all the sound energy of the open test section is supplied by the reverberant field of these duct spaces.



The recorded impulse response curves indicate that the room acoustic of the open test section is very complex. The insights gained about the nature of the power flow in the tunnel, by studying the impulse responses and the spatial distribution of sound for a steady-state sound source, are significant. However, much more information could be obtained by using a small-scale model of the tunnel where systematic experimentation could be carried out at low cost and without interference of the on-going test program in the V/STOL Tunnel. The results of such a scale-model study would not only provide information valuable for the proper planning of acoustical experiments in the V/STOL Tunnel and other tunnels of similar geometry, but also would yield information which would be useful for the planning of new wind tunnels to be used for acoustic testing.

## VII. PREREQUISITES FOR PERFORMING VALID ACOUSTICAL MEASUREMENTS IN THE OPEN TUNNEL TEST SECTION

As already concluded from the results of the impulse response and steady-state measurements, the reverberant sound field in the open test section is far from being a truly diffuse field. Accordingly, the sound power output of an unknown source cannot be determined from the space-averaged sound pressure level measured in the reverberant field. The only practical way to measure the sound power output and directivity pattern is to perform sound pressure measurements on the surface of an imaginary sphere centered on the source location and having a radius within which the microphone is capable of measuring the direct sound with sufficient accuracy. The total sound power output of the source is then obtained by integrating the squared rms sound pressure over the total solid angle  $4\pi$ ; namely,

$$W_0 = \frac{r^2}{\rho_0 c_0} \int_{\phi=0}^{2\pi} \int_{\theta=0}^{\pi} p_{rms}^2(\phi, \theta, r) \sin\theta \, d\theta d\phi, \quad (6)$$

where  $p_{rms}(\phi, \theta, r)$  is the rms sound pressure of the direct sound, measured in distance  $r$  from the acoustical center of the source and in the direction defined by the polar angle  $\phi$  and elevation angle  $\theta$ .

To assure that the microphone measures the direct sound, the following conditions must be fulfilled simultaneously:

1. The measuring distance  $r$  must be small enough that the contribution of the reverberant field is negligible.

2. The intensity of the direct sound must be large compared with the self-noise of the tunnel.
3. The microphone output due to the flow-induced pressure fluctuations must be small compared with the output signal due to the true sound field.

Assuming that the directivity of the source's radiation pattern is less or equal to that of the microphone and the required accuracy is 1 dB, Condition 1 is usually fulfilled if the measuring distance is equal to or smaller than the half hall radius. Since the average hall radius of the V/STOL Tunnel is 16 ft, the measuring distance would be in the order of 8 ft or smaller.

The data plotted in Figs. 2, 3, 4, 7, and 8 provides the necessary information to predict the self-noise with an accuracy sufficient to make an estimate whether Condition 2 will be fulfilled or not.

It is very difficult to determine whether or not the microphone signal is masked by flow-induced pressure fluctuation because the present state of the art in designing microphones with low sensitivity to convected pressure fluctuations is in the early stage of development. We have been fortunate indeed to have the opportunity to use in our experiments one of the first porous-pipe microphones which have this capability of partially cancelling the effect of convected pressure fluctuations. Without this microphone, data obtained in the presence of flow would have been incorrect. Unfortunately, the porous-pipe microphone as presently constituted possesses this flow noise rejection capability only if oriented exactly

parallel to the flow. For other angles of orientation, the porous-pipe microphone does not possess any flow noise rejection capability. Accordingly, if we want to advance our knowledge as to how the presence of the flow influences sound generation, the development of microphones which have flow noise rejection capability for all angles of orientation in the flow must have high priority.

### VIII. OBSERVATIONS MADE WITH THE CLOSED TEST SECTION CONFIGURATION

Though not required by the present contract, we made some preliminary measurements for the closed test section configuration of the tunnel. We were motivated to do so because we suspected that the closed test section configuration might offer a simpler means to measure the power output of an unknown source than would the open test section configuration. We also expected to gain some information about the process by which the acoustic power is distributed within the various sections of the closed tunnel.

We placed our semi-omnidirectional loudspeaker source in the center of the closed tunnel test section 7 ft and 10 in. above the floor and measured the octave band sound pressure level in the upstream and downstream direction as a function of distance. The speakers were fed by a constant voltage of 8 V<sub>rms</sub>. The tunnel, during these measurements, was stationary.

The measured data for the downstream traverse are plotted in Fig. 15, which also shows a sketch of the measurement set-up. Figure 15 indicates that there is very little attenuation with increasing distance, because all sound energy radiated by the source in the downstream direction remains confined in the duct. The small attenuation is due partly to the expansion of the duct cross section and partly to the loss of power through the duct walls and air absorption (the latter increasing with increasing frequency). The most substantial loss occurs across the turning vanes, which provide a partial shielding. Though the measurements were restricted to a single location

at each measuring point, they may provide a fair estimate for the space average across the entire duct cross section, since the pressure was found to be quite evenly distributed.

Figure 16 shows the data obtained for the traverse in the upstream direction. Because our sound source was omnidirectional and the cross section of the test section is substantially the same in both directions, the octave band sound pressure levels measured at 25 ft and 50 ft from the source agree well with those measured in the downstream direction. The levels measured at 115 ft distance, however, are considerably smaller than those measured for the same distance in the downstream direction, because of a substantially larger tunnel cross section at the upstream side. It is reasonable to assume that the measured levels would have been different if the sound source had had a strongly directional radiation pattern, though this was not checked experimentally.

From the limited data available, it seems likely that the closed tunnel configuration would provide a more practical means of evaluating the sound power output of an unknown sound source than would the open test section configuration. It is likely that the measurement of the sound pressure level in an upstream and downstream location would be sufficient to calculate the power output. In these locations (i.e., inside the duct), one could retain the orientation of a porous-pipe type microphone parallel to the flow, which is necessary to take advantage of its flow noise cancellation capabilities.

Therefore, we recommend that the feasibility of performing valid acoustical measurement in the closed configuration of the V/STOL Tunnel should be studied on a scale model of the tunnel.

## IX. RECOMMENDATIONS

The following recommendations are based on the information provided by this study:

1. Noise control measures should be undertaken to reduce the level of the boundary layer suction fan noise at least 6 dB below the level of the driving fan noise in each octave band.
2. The feasibility of making valid sound power measurements in placing the source in the closed tunnel test section should be investigated both theoretically and experimentally. The majority of the experimental work should be conducted in a scale-model of the V/STOL Tunnel. Studying the acoustics of the tunnel on a scale model, instead of in full-scale, has the advantage that systematic changes can be undertaken to evaluate their effect and that the testing work conducted in the V/STOL Tunnel would not be disturbed.
3. The feasibility of reducing driving fan noise in the test section by applying acoustical wall treatment or inserting silencers at strategically located points of the tunnel should be studied. A reduction of the driving fan noise would be necessary to enable one to measure the sound radiation of sources of moderate sound power output. A scale model, we think, would provide the most practical means for such a study.
4. Research and development work directed toward the design of microphones with flow noise rejection capability should be encouraged. Directional microphones with a flow noise reduction capability, which is independent of their orientation in respect to the flow, are essential to making valid acoustical measurements in the presence of flow.

## REFERENCES

1. Vér, I.L., C.I. Malme, and E.B. Meyer, "Acoustical Evaluation of the NASA Langley Full-Scale Wind Tunnel," BBN Report 2100, January 1971 (NASA CR 111868).
2. Bruel, P.V., "Aerodynamically Induced Noise of Microphones and Windscreens," Bruel & Kjaer Technical Review, No. 2, 1960.
3. Noiseux, D.U. and T.G. Horwath, "Design of a Porous Pipe Microphone for the Rejection of Axial Flow Noise," Paper CC8, Presented at the 79th Meeting of the Acoustical Society of America in Atlantic City, 23 April 1970.
4. Vér, I.L., "Acoustical Modeling of the Test Section of the NASA Langley Research Center's Full-Scale Wind Tunnel," BBN Report No. 2280, 30 Nov. 1971.
5. Bies, D.A., "Investigations of the Feasibility of Making Model Acoustic Measurements in the NASA Ames 40-by-80 Foot Wind Tunnel," BBN Report No. 2088, July 1970.



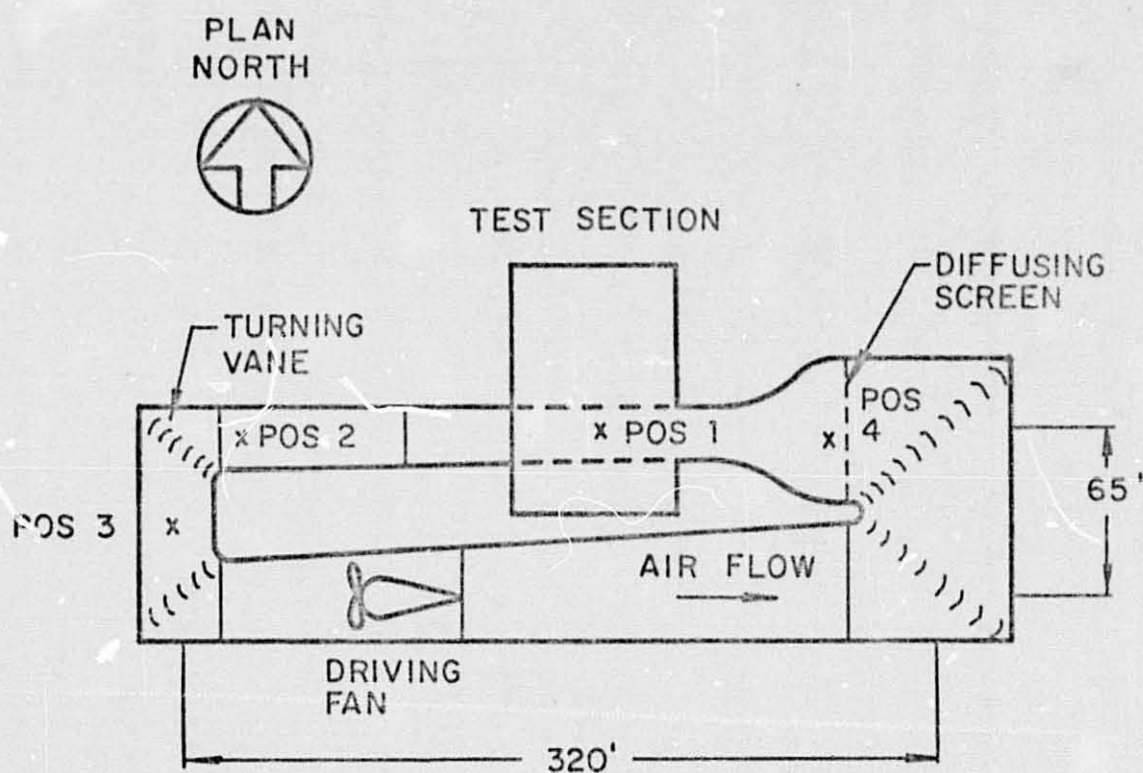


FIG. 1. PLAN VIEW OF THE V/STOL WIND TUNNEL

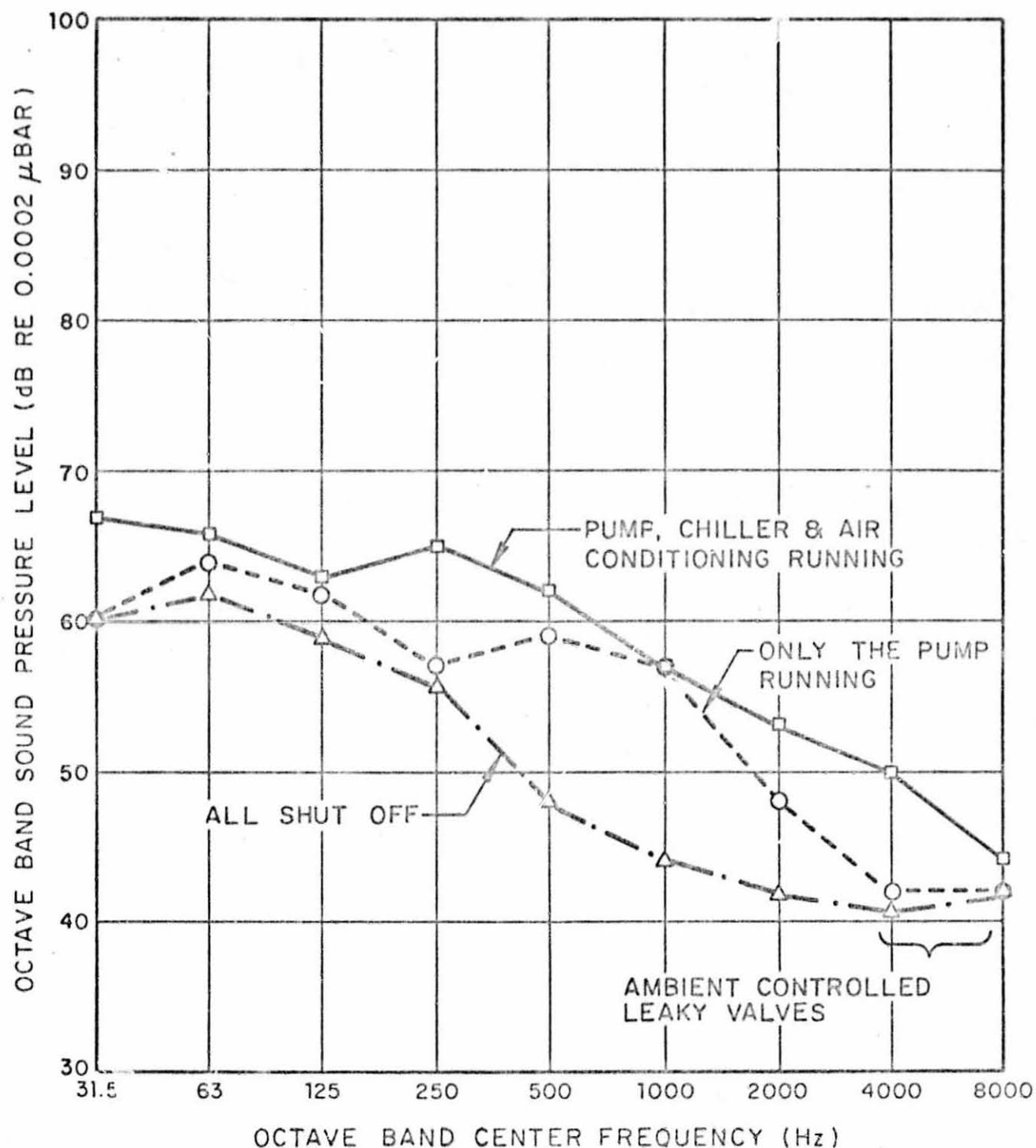


FIG. 2. OCTAVE BAND SPECTRUM OF THE AMBIENT NOISE IN THE OPEN TEST SECTION WITH TUNNEL FAN STATIONARY

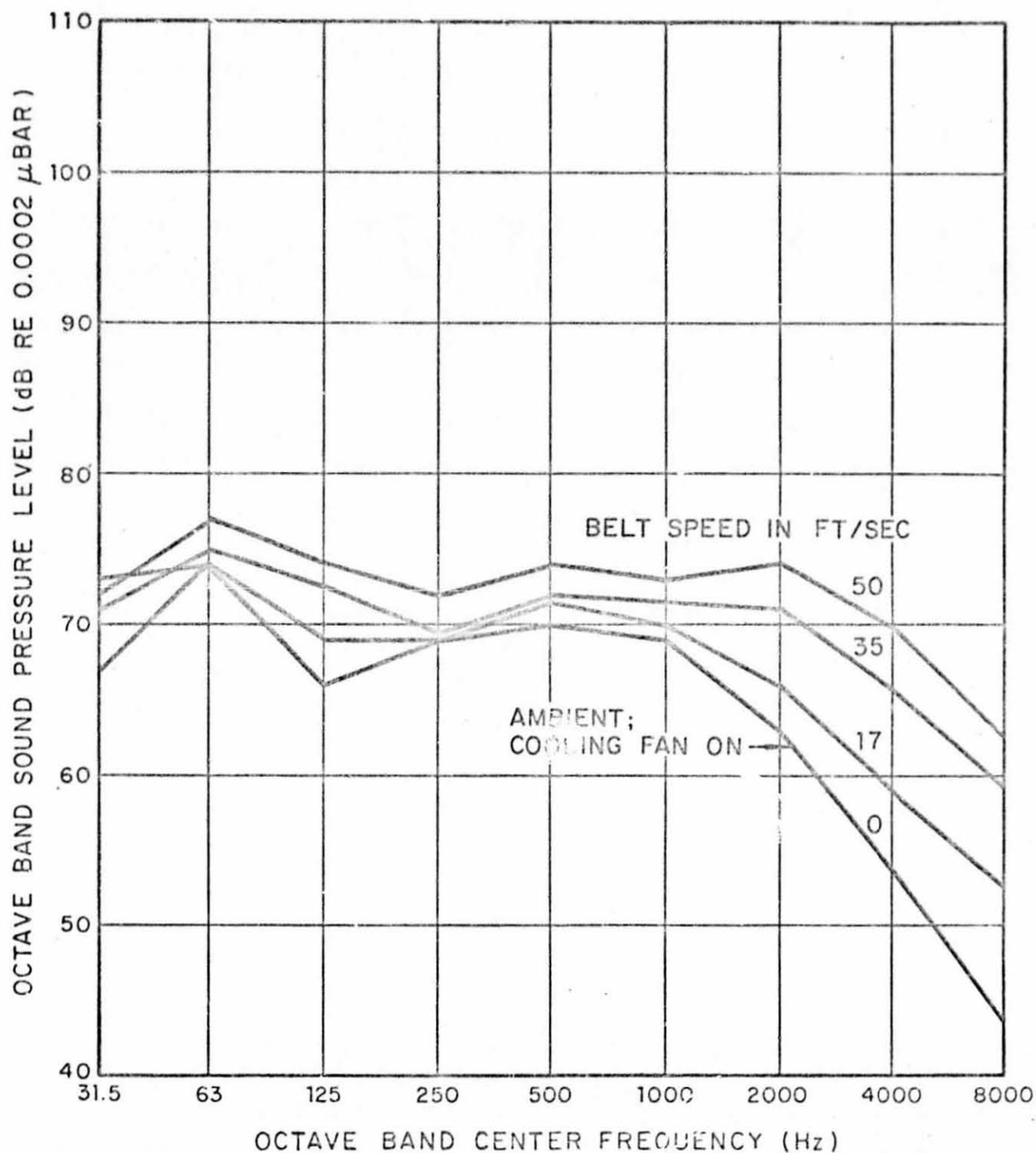


FIG. 3. OCTAVE BAND SPECTRUM OF THE GROUND BELT SYSTEM MEASURED AT 3 FT FROM THE DOWNSTREAM END OF THE BELT

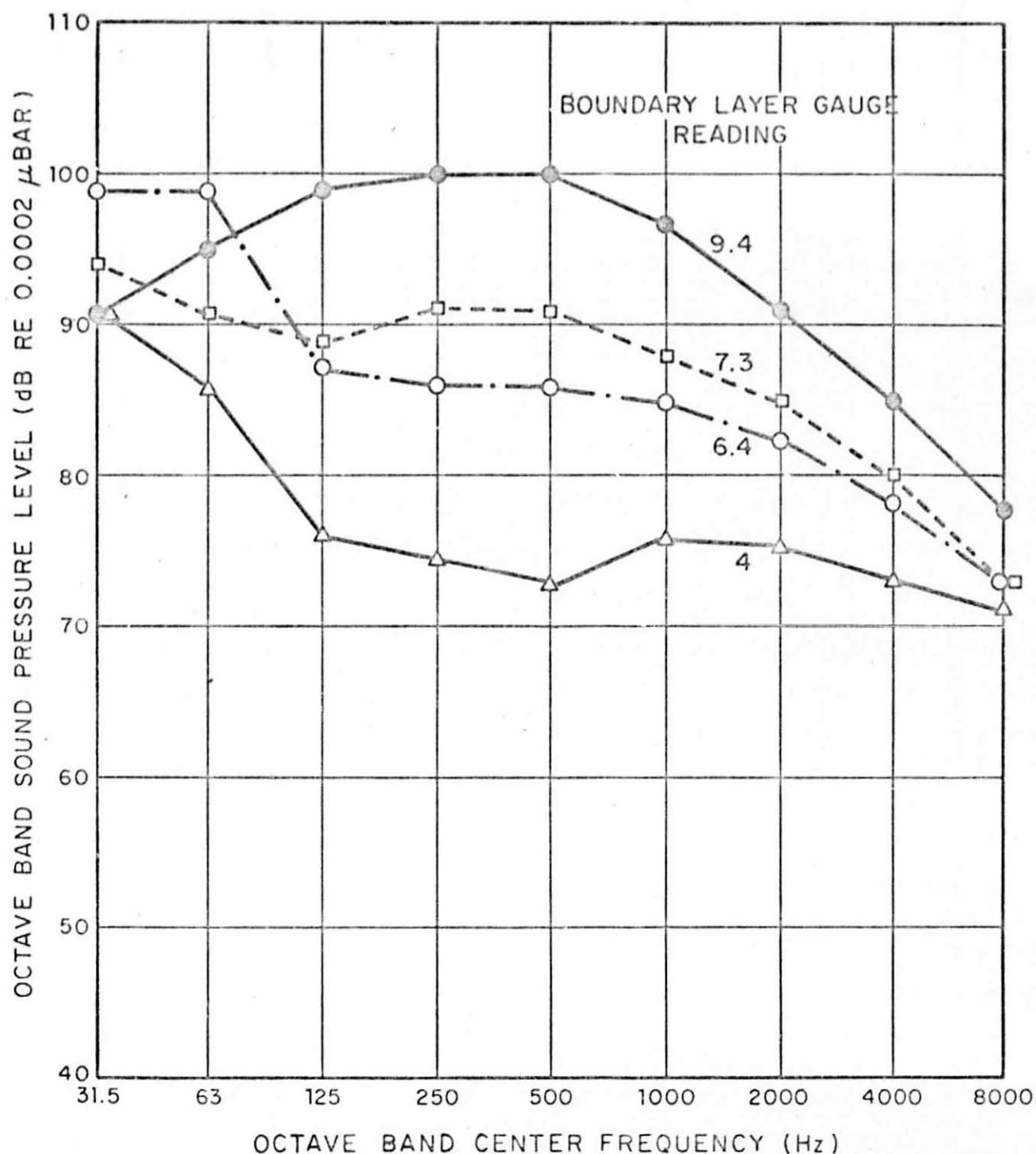


FIG. 4. OCTAVE BAND SPECTRUM OF THE BOUNDARY LAYER SUCTION FAN NOISE IN THE OPEN TEST SECTION WITH THE TUNNEL FAN STATIONARY

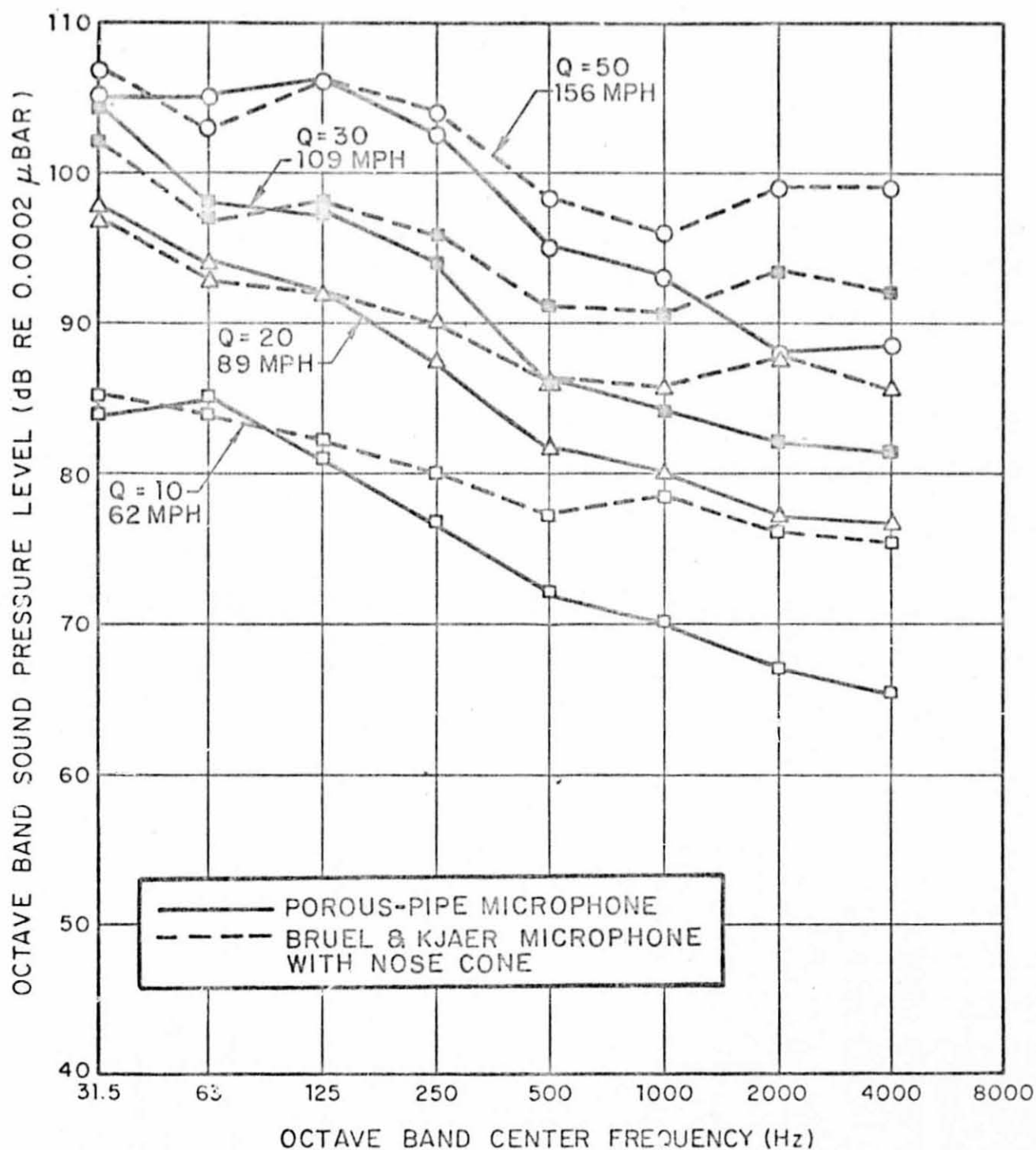


FIG. 5. COMPARISON OF THE FAN NOISE LEVELS MEASURED IN THE STREAM BY TWO DIFFERENT MICROPHONES

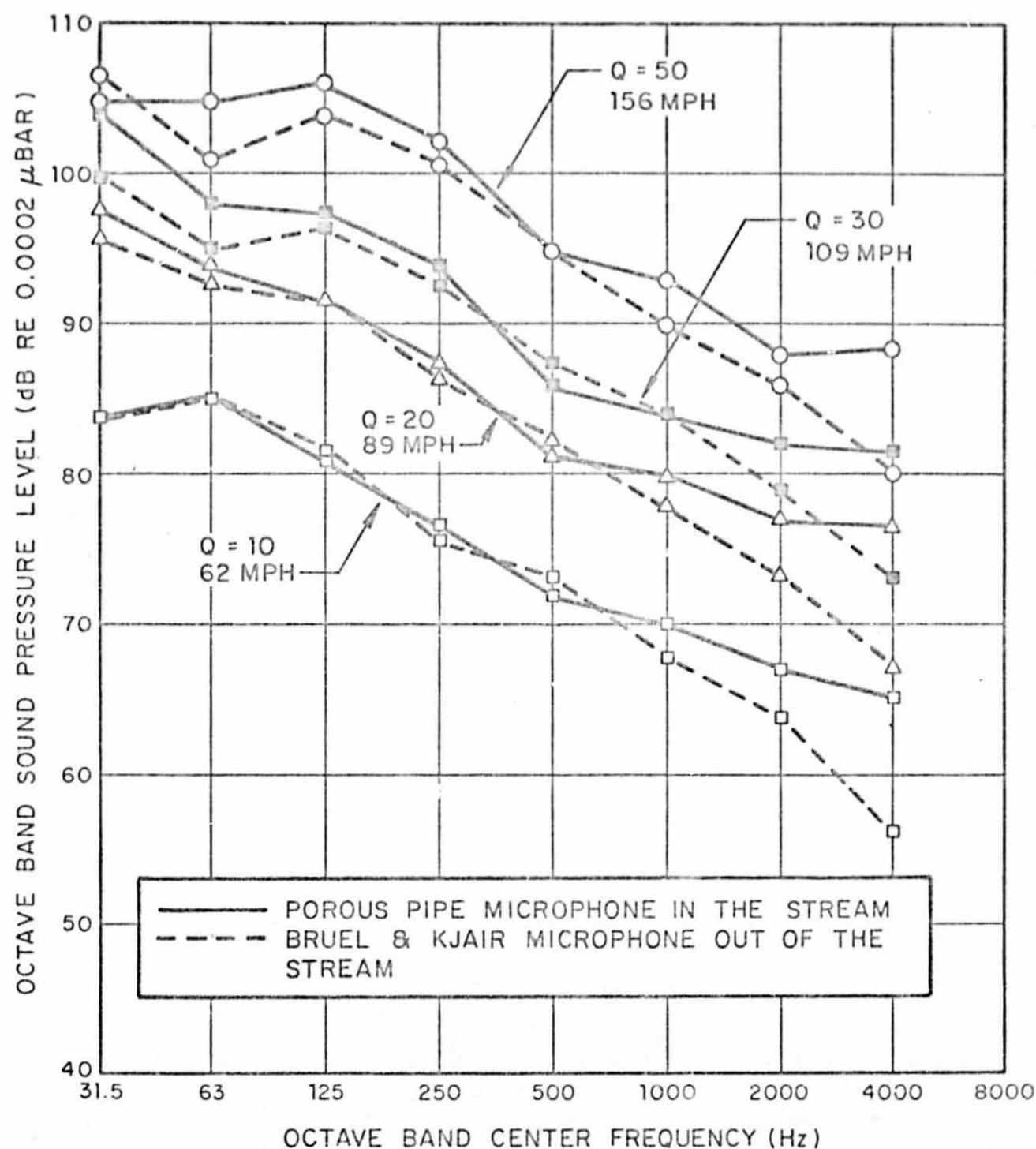


FIG. 6. COMPARISON OF THE FAN NOISE LEVELS IN THE TEST SECTION MEASURED IN AND OUT OF THE STREAM

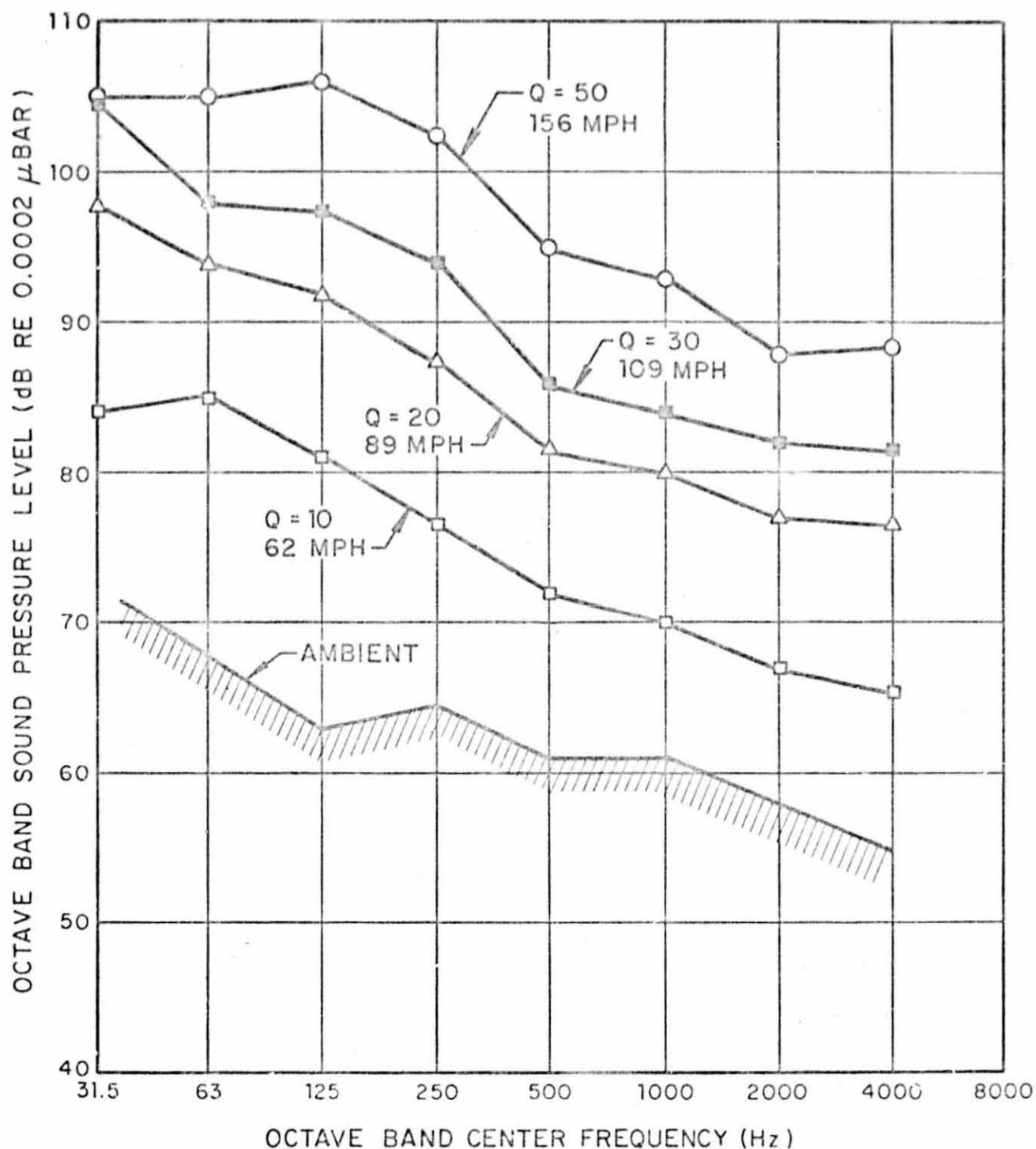


FIG. 7. OCTAVE BAND SPECTRUM OF THE DRIVING FAN NOISE IN THE TUNNEL TEST SECTION MEASURED WITH THE POROUS PIPE MICROPHONE WITH AIR SPEED AS PARAMETER

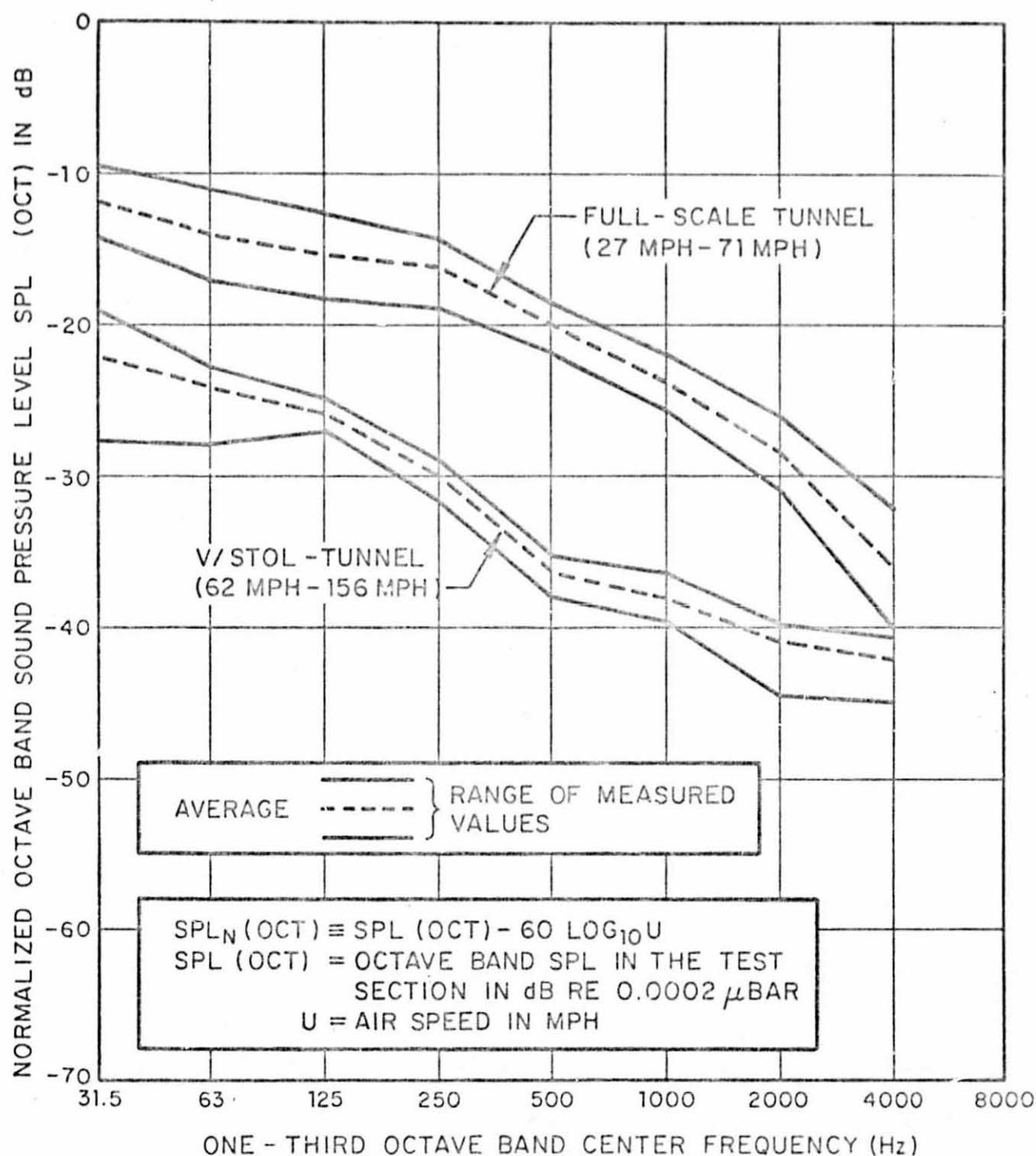


FIG. 8. NORMALIZED OCTAVE BAND SOUND PRESSURE LEVEL OF THE V/STOL AND FULL-SCALE WIND TUNNELS DUE TO THE OPERATION OF DRIVING FANS



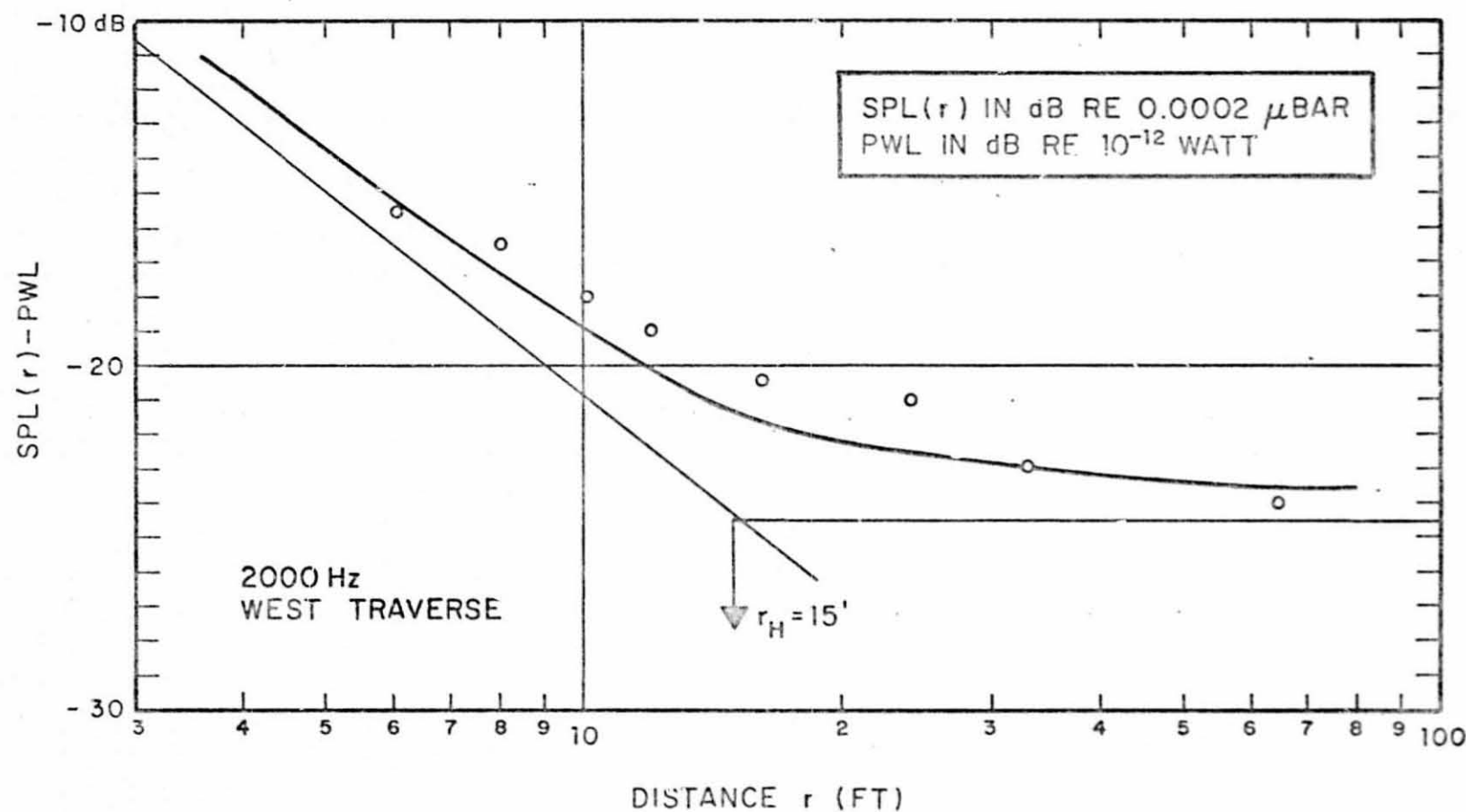


FIG. 9. EXAMPLE FOR THE EVALUATION OF THE HALL RADIUS FROM MEASURED SPL VS DISTANCE CURVES BY THE BEST-FIT METHOD

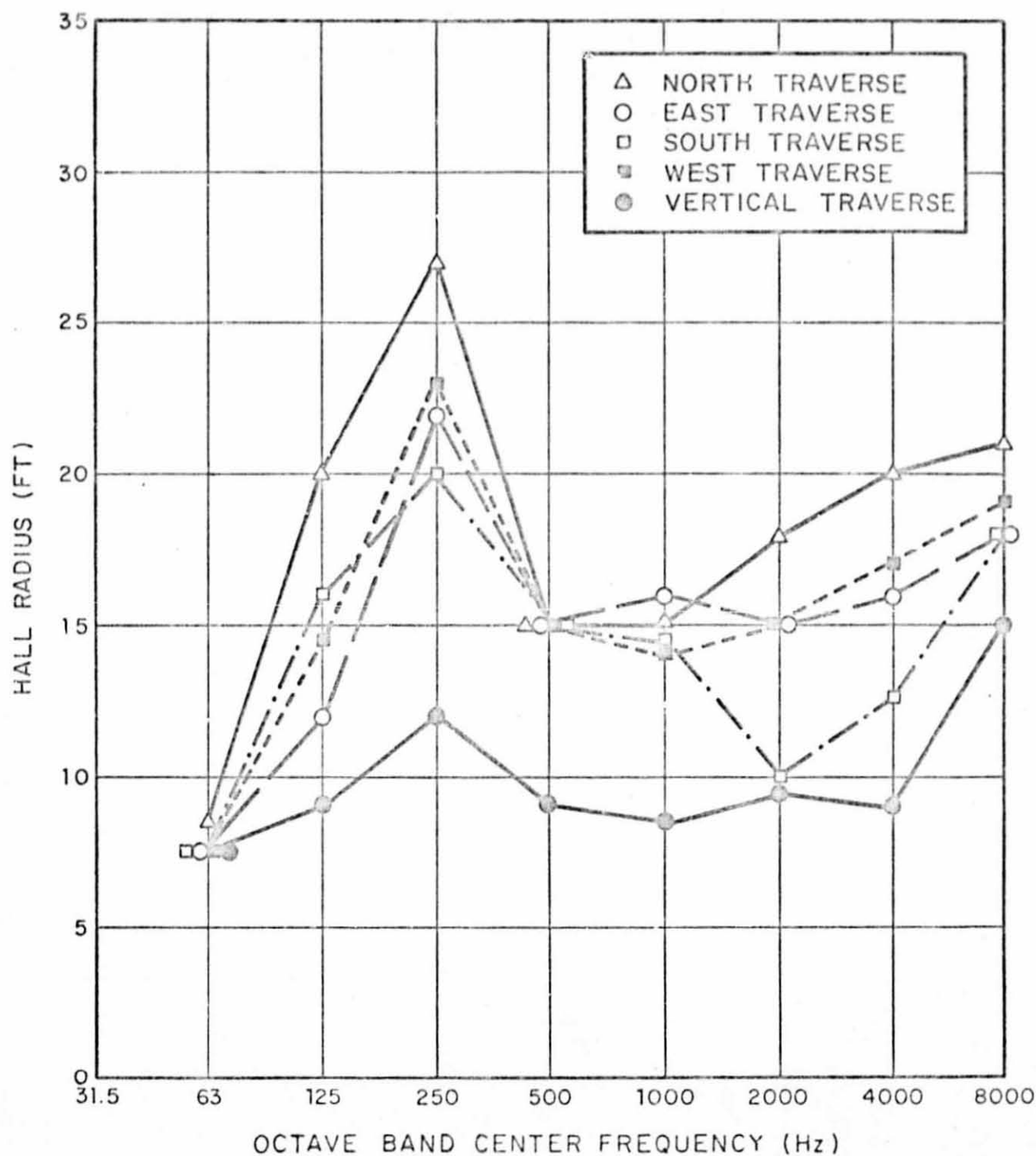


FIG. 10. HALL RADIUS OF THE OPEN TEST SECTION FOR THE VARIOUS DIRECTIONS

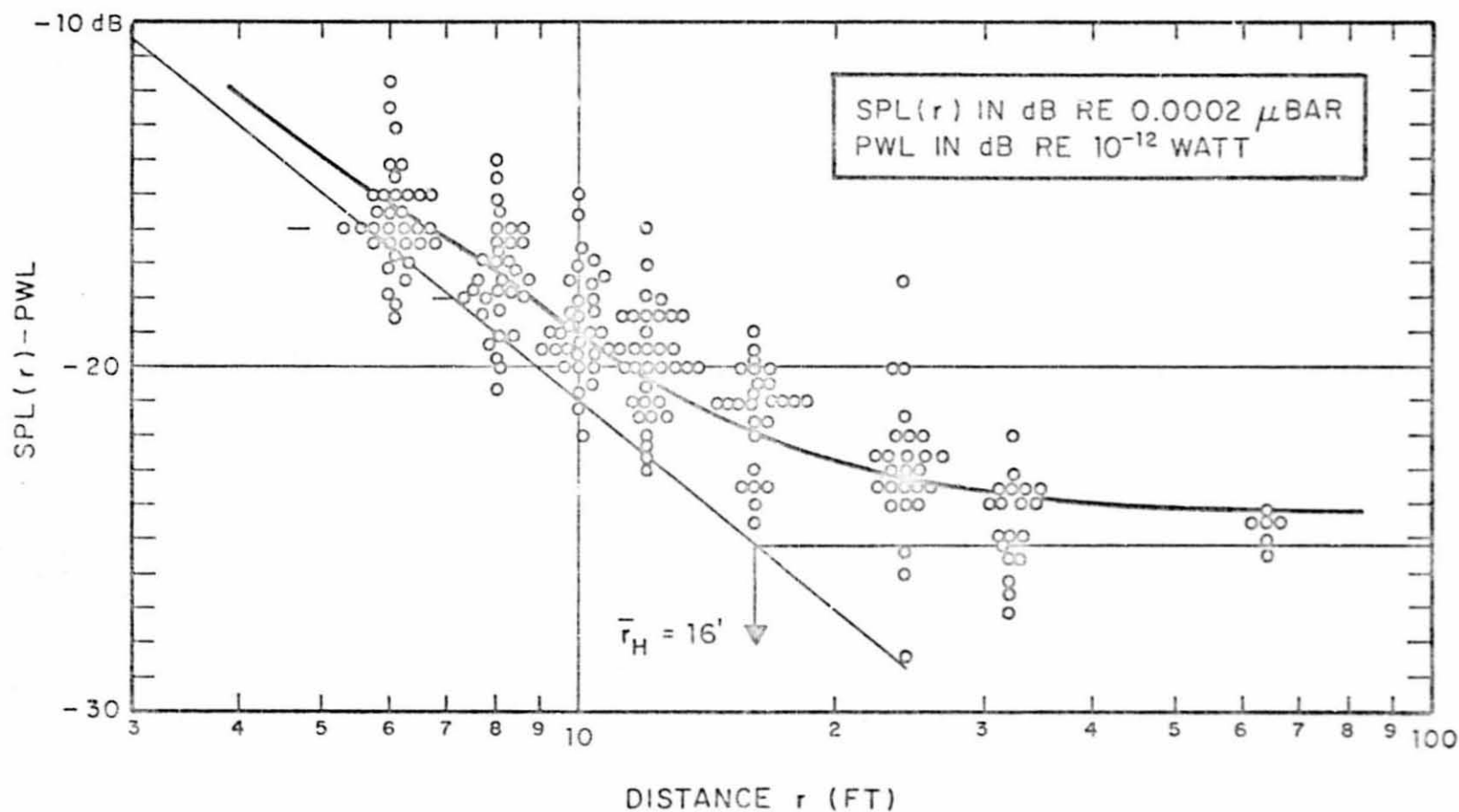


FIG. 11. DISTRIBUTION OF THE NORMALIZED SOUND PRESSURE LEVEL VS DISTANCE DATA IN THE OPEN TUNNEL TEST SECTION FOR ALL FREQUENCIES AND ALL DIRECTIONS

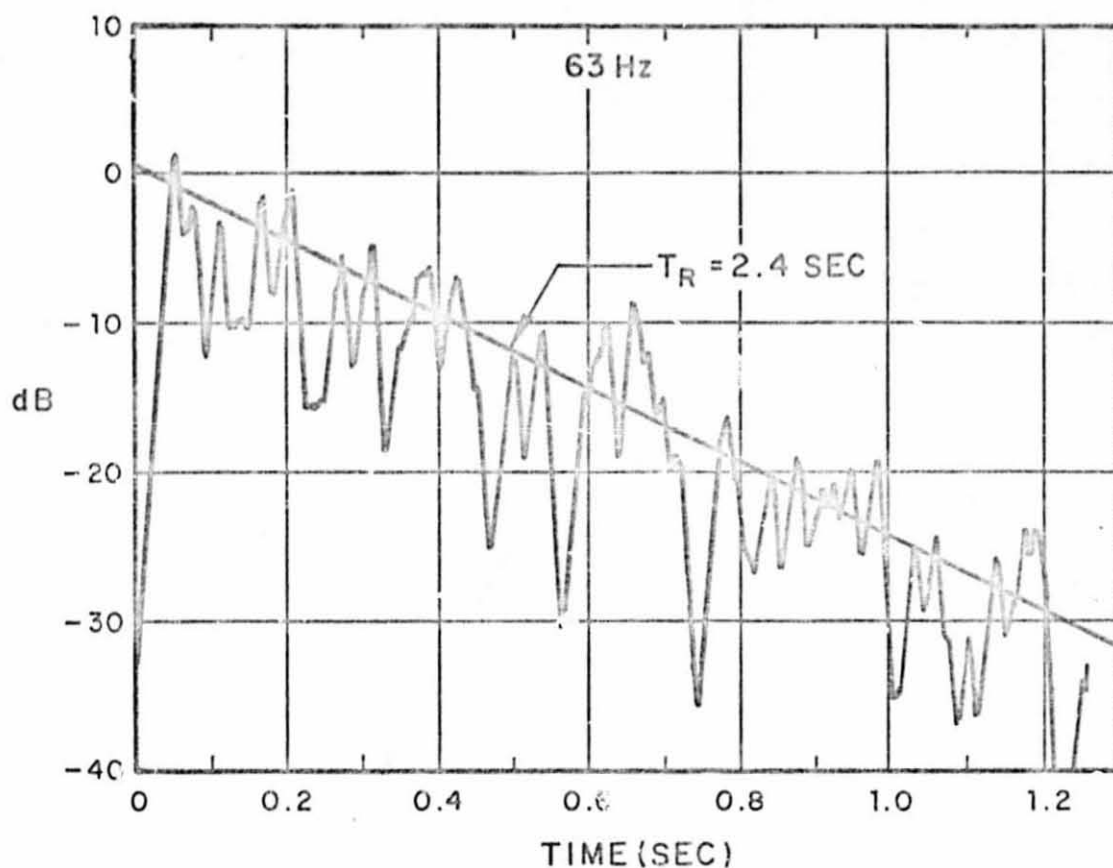


FIG. 12. IMPULSE RESPONSE OF THE OPEN TUNNEL TEST SECTION MEASURED IN THE 63-HZ CENTER FREQUENCY OCTAVE BAND

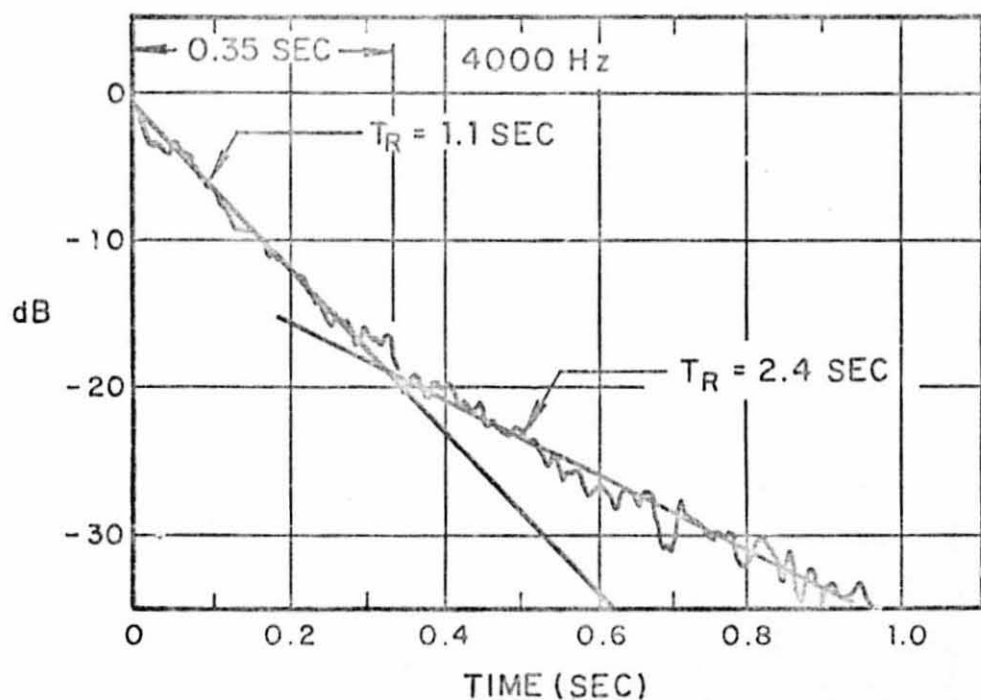
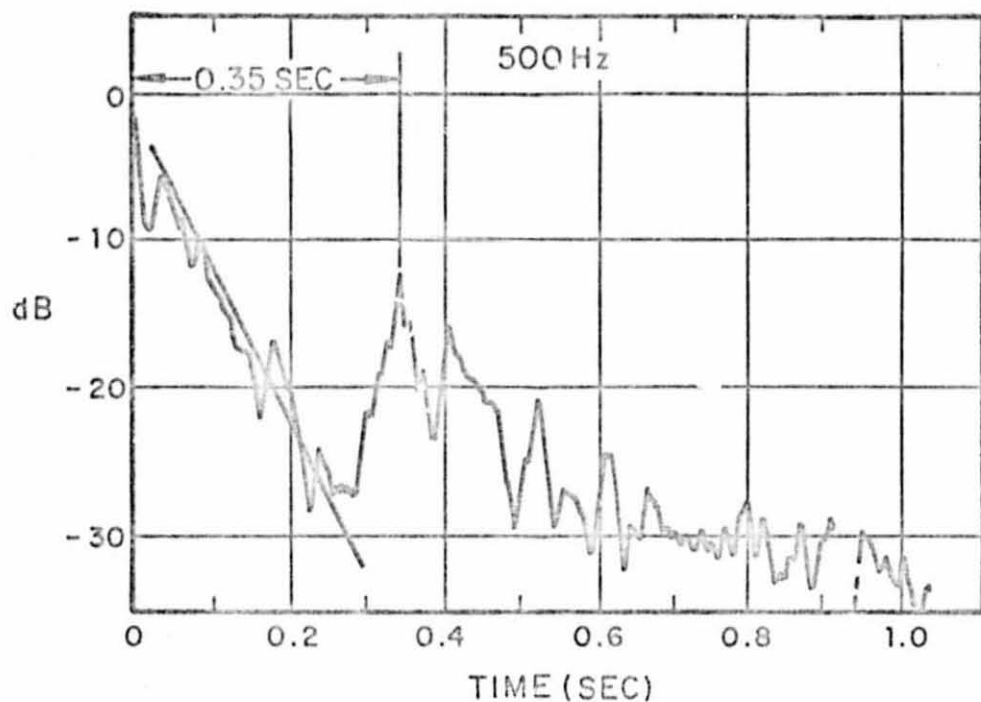


FIG. 13. IMPULSE RESPONSE OF THE OPEN TUNNEL TEST SECTION  
RECORDED IN THE 500-HZ AND 4000-HZ CENTER  
FREQUENCY OCTAVE BANDS

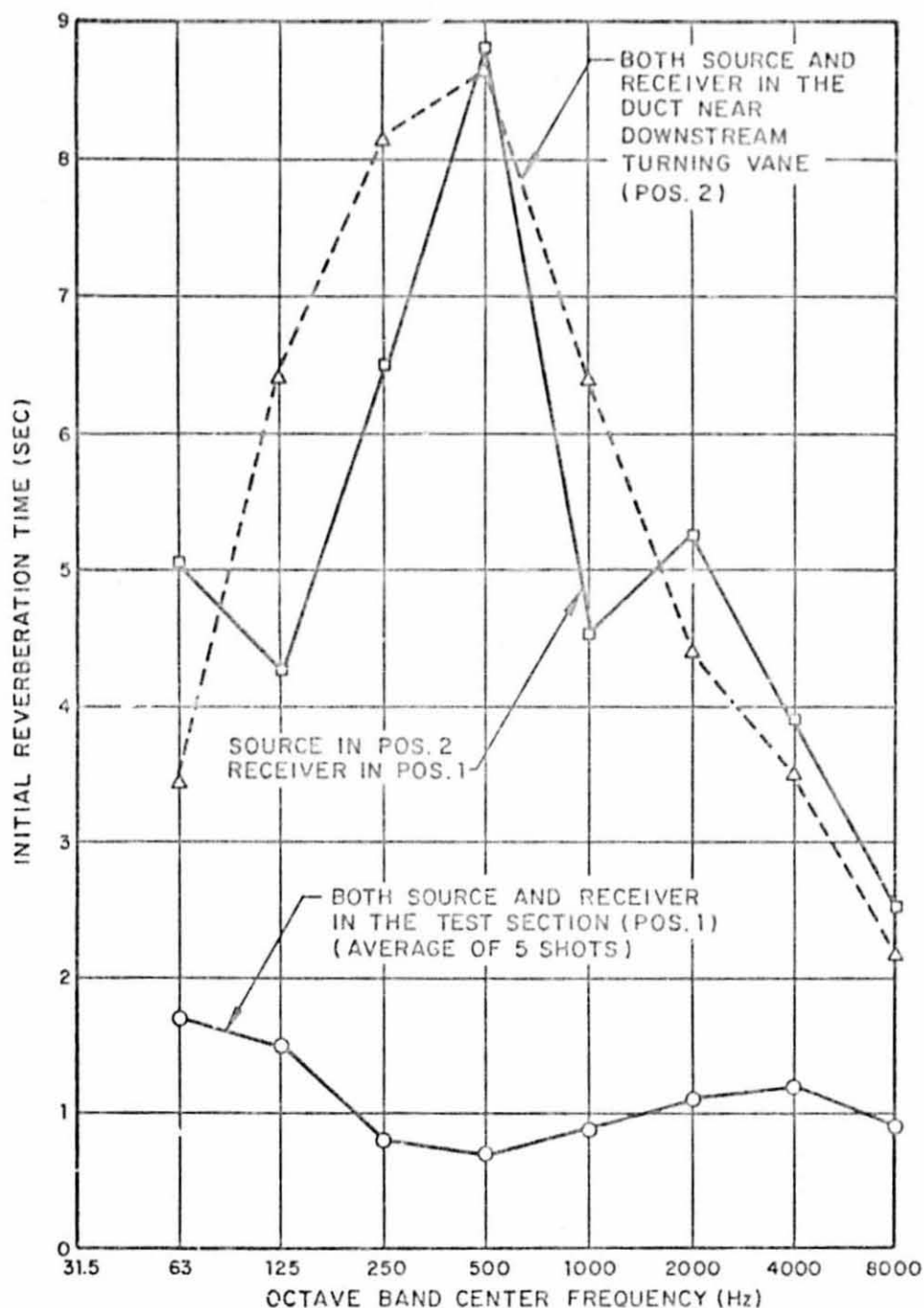


FIG. 14. INITIAL REVERBERATION TIMES MEASURED WITH VARIOUS SOURCE AND RECEIVER LOCATIONS

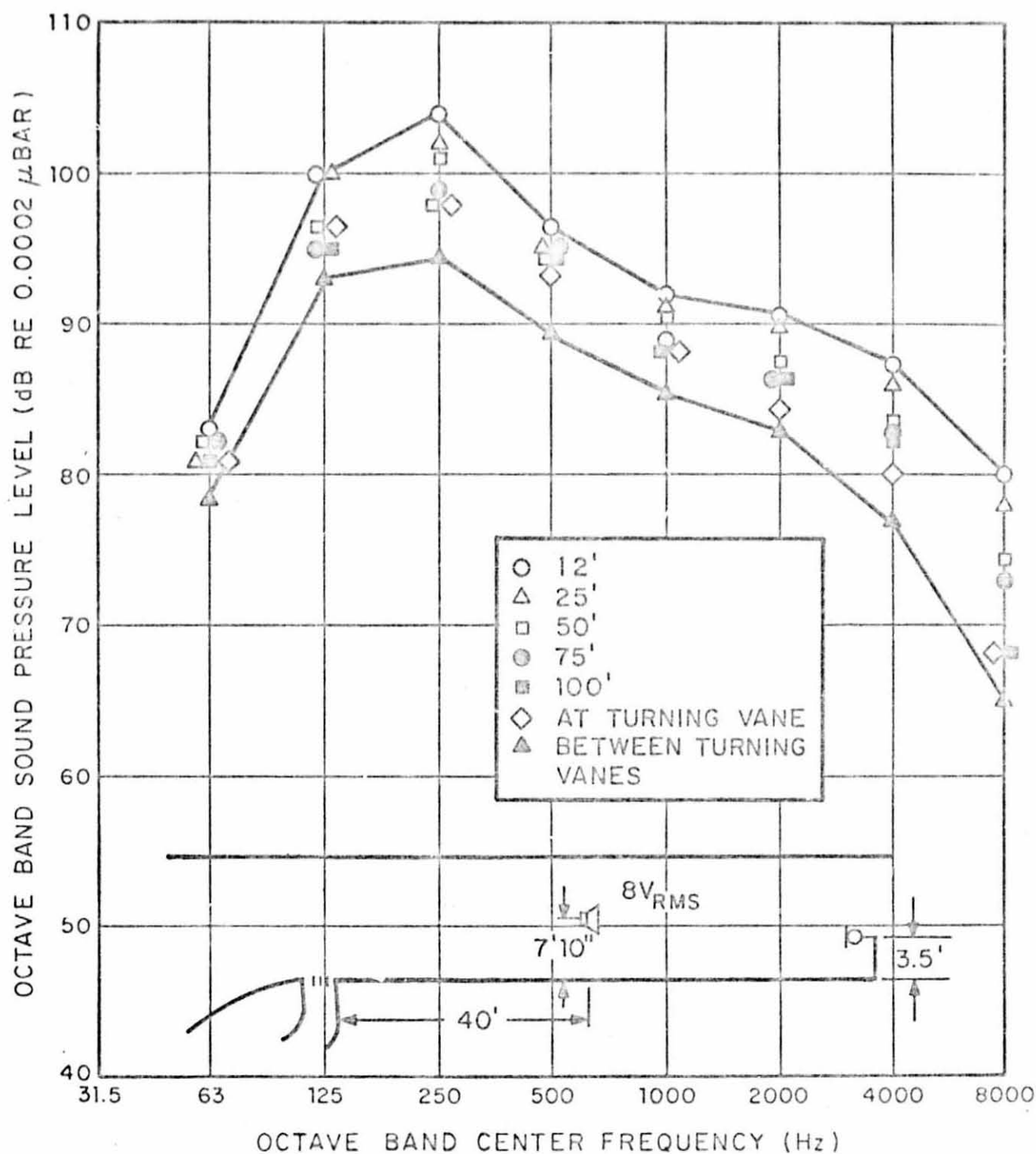


FIG. 15. SPL VS DISTANCE MEASURED IN THE DOWNSTREAM DIRECTION  
IN THE CLOSED V/STOL TUNNEL

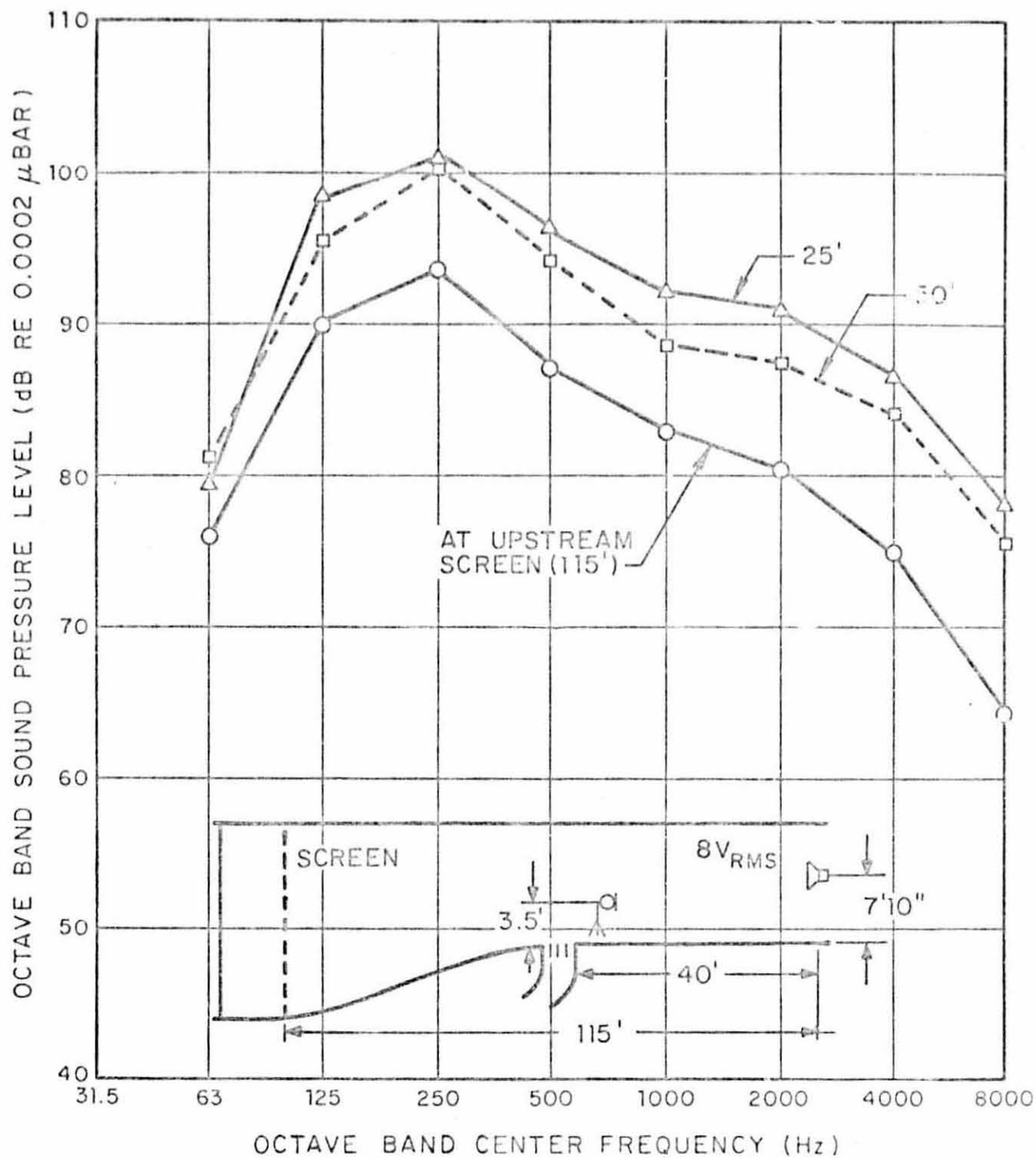


FIG. 16. SPL VS DISTANCE MEASURED IN THE UPSTREAM DIRECTION IN THE CLOSED V/STOL TUNNEL